

LIDAR DATA PRODUCTS AND APPLICATIONS ENABLED BY CONICAL SCANNING

Geary K. Schwemmer⁽¹⁾, David O. Miller⁽²⁾, Thomas D. Wilkerson⁽³⁾, Sangwoo Lee⁽²⁾

⁽¹⁾ NASA, Code 912 Greenbelt, MD 20771, USA. Email: Geary.K.Schwemmer@nasa.gov

⁽²⁾ Science Systems and Applications Inc., Code 912 Greenbelt, MD 20771, USA

⁽³⁾ Space Dynamics Laboratory, Utah State Univ., SER Bldg. Logan, UT, 84322-4405, USA

ABSTRACT

Several new data products and applications for elastic backscatter lidar are achieved using simple conical scanning. Atmospheric boundary layer spatial and temporal structure is revealed with resolution not possible with static pointing lidars. Cloud fractional coverage as a function of altitude is possible with high temporal resolution. Wind profiles are retrieved from the cloud and aerosol structure motions revealed by scanning. New holographic technology will soon allow quasi-conical scanning and push-broom lidar imaging without mechanical scanning.

1. CONICAL SCANNING TECHNOLOGY

Airborne and spaceborne scanning lidars address the need to spatially sample a target perpendicular to the ground track in order to get a 3-D data set. Conical scanning is simpler and more compact than most other methods of cross-track scanning, especially when scanning a large aperture over angles greater than about 10°. For Doppler wind measurements, scanning is used to sample the atmosphere from different directions in order to retrieve orthogonal horizontal components of the wind field.

A conventional scanning lidar usually employs a transceiver telescope mounted on a 2-axis az-el mount or a fixed transceiver with 1 or 2 scanning flat mirrors to direct the laser and receiver field-of-view (FOV). Conical scanning has been contemplated for spaceborne lidars but otherwise is not often used. However, fixed-elevation azimuthal scanning is the typical mode of operation of Doppler radars. For ground-based radar, the elevation axis is kept low near the horizontal since the primary scatterers, insects or hydrometeors, are mostly in the boundary layer (BL). Simplified conical scanning for lidar is achieved using a rotating holographic optical element (HOE) in the Holographic Airborne Rotating Lidar Instrument (HARLIE) [1]. The elevation angle is fixed in the HOE, and the rotation axis usually positioned vertically toward zenith for ground-based operation and toward nadir for airborne applications.

Conical scanning from a ground-based platform generates a time series of measurements over the same 2-D conical surface through which the atmosphere advects. One can observe not only the spatial variations

of whatever is being measured over any one scan, but one also can describe temporal variations with fairly high resolution, on the order of seconds.

2. BOUNDARY LAYER STRUCTURE

Scanning lidar is particularly well suited for studying the atmospheric BL due to its complex dynamics in space and time on all scales. For example, we will describe BL structure observed with HARLIE on 14 June 2002 during the IHOP field experiment, near Balko, Oklahoma in the Central Great Plain of the US (36° 33.500' N, 100° 36.371' W, Alt 850 m). HARLIE was continuously scanning 360° in azimuth with a fixed 45°-elevation angle. A conventional backscatter time-height image for this time period is shown in Fig. 1, where altitude is plotted on the Y-axis, time on the X-axis and the \log_{10} of range-squared corrected backscatter ($R^2\beta_{\pi}$) is represented in intensity (color). We averaged backscatter profiles over about 5 consecutive scans (1 minute) to generate Fig. 1. The height of the BL is calculated on the one-minute data and plotted as a white line on the image. Sunrise occurs about 1100 UT, and the BL is observed to grow slowly from its nocturnal level. At the same time, an overlying scattering layer is slowly descending. Backscatter in the BL is thick and fairly uniform until about 1540 UT, when it begins to rise more quickly and displays increasing variability. At the same time, the average backscatter level within the BL is decreasing. Convective plumes are evident after 1600 UT, and weak clouds can be seen capping them beginning after 1740 UT. But this representation does not give any indication of the horizontal scale of the plumes, unless

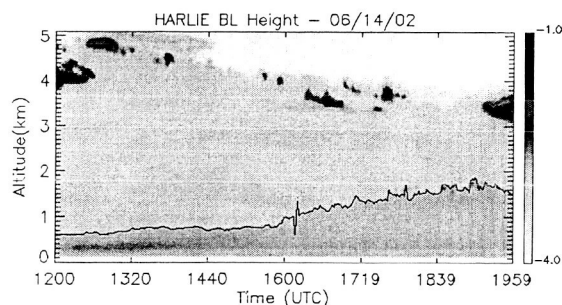


Fig. 1. Time (X) - height (Y) image of \log_{10} range corrected backscatter on 14 June 2002 near Balko, OK during IHOP.

one knows the speed at which the BL air (and presumably the plumes) advects over the site. The region between the tops of the thermals and the valleys of subsiding air in between is an entrainment zone (EZ) and an important parameter in BL models. To measure this with a vertical pointing lidar one needs the statistics of these differences over several peaks and valleys, which in this case could take more than an hour during which the BL may undergo significant evolution. The scanning data can be analyzed to provide both the horizontal spatial scale of the convective plumes as well as the EZ thickness within seconds.

On 14 June, HARLIE was scanning at 5 RPM, acquiring backscatter profiles with a 1-watt, 5 KHz

rep-rate, 1064 nm Nd:YAG laser. Shots are integrated every 100 ms, or 3° in azimuth, 120 profiles per scan. We compute the BL height on each 100 ms profile and the mean and standard deviation for each scan. The standard deviation (σ) of BL height is one measure of EZ thickness. The top of Fig. 2 displays BL height as a function of azimuth (Y-axis) and time (X-axis). Image intensity (color) is proportional to the BL height, assigned using the color bar on the right, and varies between 636 and 2015 m. Below the image we plot the mean and σ of the BL height as a function of time. The most striking feature in this space-time representation of BL height is how smooth the BL is between 1200 and 1600 UT and how rough it becomes after that, which is incidentally about the time it converges with

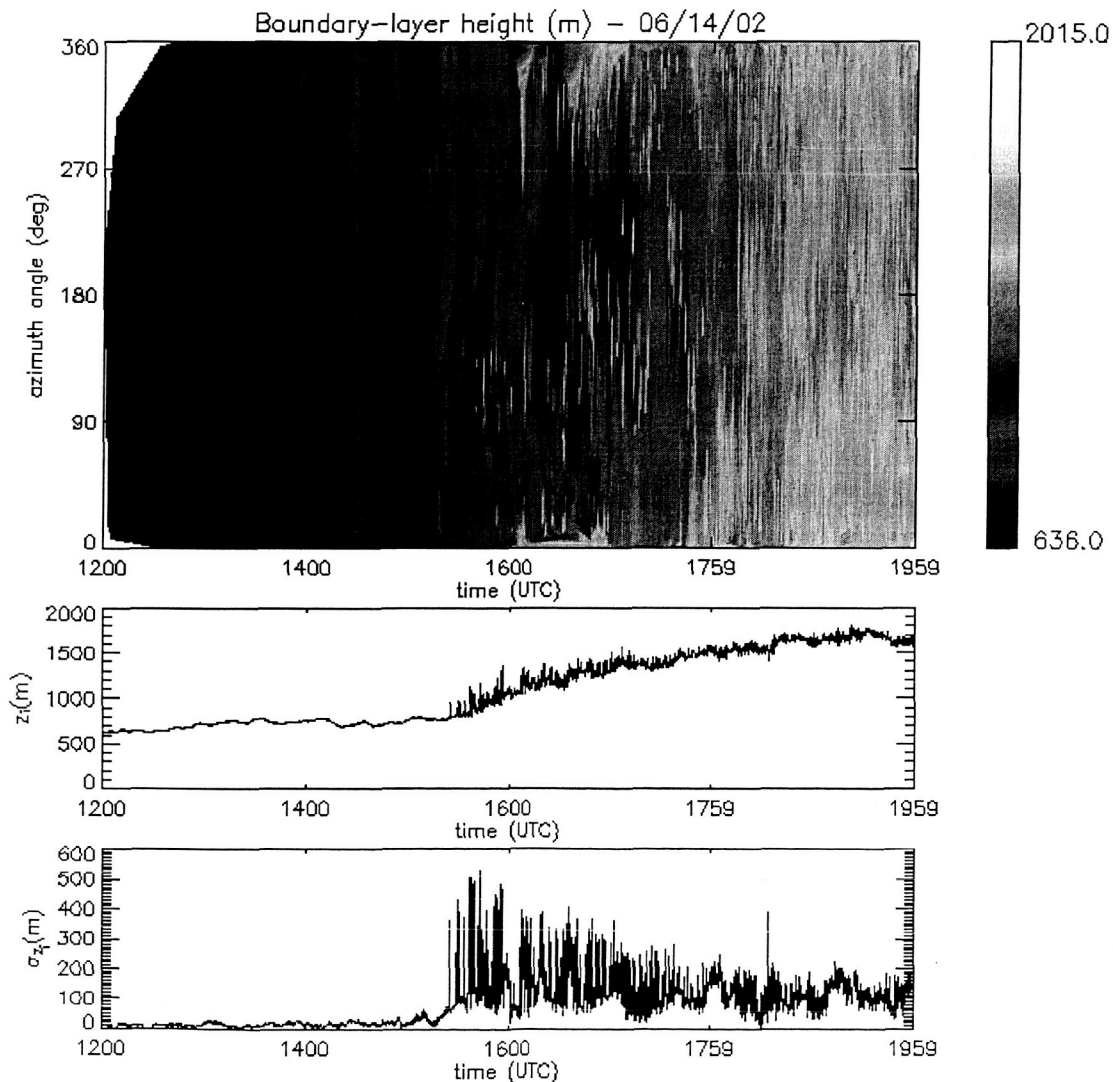


Fig. 2. *Top*- BL height (color scale) plotted as a function of time (X) and azimuth (Y); *Middle*- mean BL height per scan; *Bottom*- BL height standard deviation per scan.

the residual, presumably moist, layer above. Before 1600 UT the BL top is seen to undulate up and down about 100 m in a more or less uniform fashion across the scan. There is no structure in the azimuth at this time, indicating the waves are either stationary or moving slowly. The BL mean height during this period is about 700 m, which means that the scan circumference at the top of the BL (and the length of the Y-scale) is about 4.4 km. Even without a numerical frequency analysis, we can see waves of two different periods during the morning hours. One period is about 36 minutes and the other is about 4 minutes. Around 1500 UT we start to see curvature in the vertical bands representing the wave peaks and troughs, indicating that the waves are propagating across the scan. We can use this information to determine the propagation direction and speed, much in the same way that cloud-tracked winds are computed from HARLIE data [2]. Just about 1530 UT we start to observe structure around the scan and a marked increase in σ , which we attribute to thermal plumes. On some scans σ is as large as 500 m. At 1600 UT the mean height of the BL is about 1 km, so the Y-axis in the color image corresponds to a 6.3km scan circumference at that altitude. The plume sizes are on the order of 1 km.

3. CLOUD COVERAGE

The same type of analysis can be applied to clouds. We divide each scan into 8 equal sectors and average all the $R^2\beta_\pi$ profiles in each sector before applying a cloud signal threshold to determine which altitude bins contain clouds. The number of cloudy sectors at each altitude is plotted in Fig. 3 for 23 May 2002.

Because scanning samples over a large area and in different directions, the lidar has a higher probability of penetrating cloud decks and detecting multiple cloud layers in a less time than a non-scanning lidar system of similar power. This data contains BL, mid-level and high altitude clouds at various times of the day. Cloud fraction along with altitude information could be very

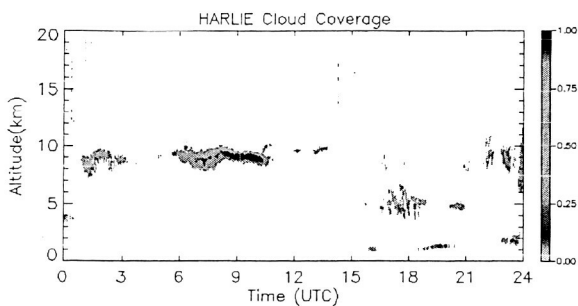


Fig. 3. Cloud fractional coverage versus time and altitude for 23 May 2002 over the IHOP Homestead site.

useful for correcting cloud-contaminated pixels in satellite spectral imager data or for parameterizing clouds in atmospheric numerical models.

4. CLOUD TRACKED WINDS

The same backscatter scanning lidar data can be analyzed to detect the motion of cloud and aerosol structures to determine the mean wind at any altitude over the scan's cone of regard. We calculated the mean wind vector at each altitude that shows significant structures in the backscatter, using techniques previously described in [2,3]. Fig. 4 is a plot of wind speed and direction for the period between 1830-1900 UT on 23 May. The HARLIE wind retrieval is successful at those altitudes where there are strong gradients in the backscatter, such as the edges of the clouds that also appear in Fig. 3. The wind profile from a GPS rawinsonde launched at the HARLIE deployment site is shown for comparison. There are also several wind retrievals from video recordings of the wide-angle SKYCAM [3].

5. DOPPLER WINDS

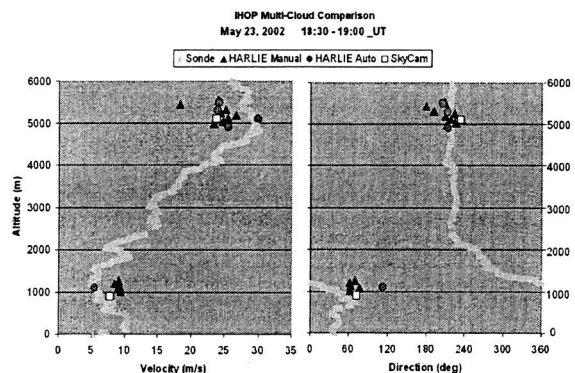


Fig. 4. HARLIE cloud-tracked winds (triangles and circles), SKYCAM winds (squares) and a coincident sonde wind profile for 1830-1900 UT on 23 May 2002 over Homestead.

Doppler wind lidar is one of the most demanding lidar applications, involving single frequency pulsed lasers, very high spectral resolution filters and large scanning telescopes. In order to retrieve a horizontal wind vector from line-of-sight Doppler measurements, observations must be made along two approximately orthogonal lines-of-sight into the same atmospheric volume. Doppler lidars have been developed mainly in two spectral regions. One is in the ultraviolet (UV) to take advantage of the large molecular scattering coefficients, and the other is in the near infrared utilizing aerosol scattering and heterodyne detectors. The later technique requires the use of diffraction-limited optics. We are currently developing HOEs for

the UV, and have proposed methods of generating similar optics for the near infrared that have diffraction limited angular resolution.

Through modeling and system design studies, a consensus has been reached by the NOAA Wind Lidar Working Group that a step-and-stare approach to scanning is preferred over continuous scanning. There are several reasons for this. One is a desire to avoid having to design lag-angle compensation and (for heterodyne lidar) wavefront tilt compensation into the transceiver. A second reason is to keep consecutive laser shots that are averaged together clustered into a smaller atmospheric volume so as not to increase the measurement variance connected with atmospheric variability over the averaging interval. However there is a penalty to pay for intermittently stopping and starting a large scanning telescope. The large inertia associated with the mass of the telescope means that it will constantly be accelerating and decelerating between pointing positions. This adds a significant dead time between successive views. In order to constantly stop and start the motion of the telescope requires a significantly larger motor than one needed to keep it rotating at a constant rate. The changing accelerations will also impart vibration and torque to the telescope, which means it has to be mechanically stiffer in order to maintain alignment. An early example of one way to avoid the complications (and costs) of such a scanning system was proposed for the BEST mission [4]. BEST was to have four fixed telescopes, each pointing in a different direction. A simple solution, but it takes four times the volume and weight of a single telescope and perhaps twice as much as a rotating telescope. For this application we are developing the lightest in large aperture scanning lidar telescopes, one without using any large moving optics. We refer to this technology as the Shared Aperture Diffractive Optical Element (SHADOE) [5]. By superimposing multiple copies of an HOE into a single holographic film, each HOE acting as a diffractive lens with its own focal plane located separately from the others, and each with a FOV aimed in a different direction, we can build a system with several independent telescopes. The beauty is that each telescope is sharing the same primary optic assembly and the same physical aperture.

We have recently experimented in the laboratory with SHADOEs containing as many as five HOEs, each separated 72° in azimuth. These devices are 20 cm in diameter, for use at 355 nm and have a 1-m focal length. The angle between the FOV and the normal is 40°, and the angle between the focus and the normal is 30°. We expect that within the next 2 years we will have 40 cm devices. In addition, we are investigating the possibility of generating aberration corrected SHADOE systems that will have near diffraction

limited focal spots for use with coherent detection Doppler lidars at 2-micron wavelengths.

6. PUSHBROOM LIDAR IMAGING

Another good application for scanning lidar is rapid topographic mapping of a planetary surface. For terrestrial commercial applications, the cost of mapping is largely dependent on the number of hours an airborne lidar takes to map a given area. The cross-track angles are not as extreme as for other lidar applications because of the rapid increase in height error due to pointing uncertainties as the scan angle becomes large. Efforts are being made at NASA to increase the swath width to 30-40° full-angle in order to minimize flight costs. These angles are difficult to achieve using a wide FOV telescope with focal plane scanning, but are very easy for a SHADOE receiver in which each HOE can have a FOV of up to 10°. The individual FOVs can be positioned so that their ground tracks form a series of adjacent parallel swaths forming one contiguous wide swath.

ACKNOWLEDGMENTS

This work was supported by Jim Dodge of NASA HQ, the NASA SBIR program, Lisa Callahan of the GSFC IRAD program, Steve Mango of the Integrated Program Office, Anel Flores of the GSFC Technology Commercialization Office, and the Space Dynamics Laboratory IR&D program.

REFERENCES

1. Schwemmer, G. K., Holographic Airborne Rotating Lidar Instrument Experiment, *19th International Laser Radar Conference*, NASA/CP-1998-207671/PT2, pp. 623-626, Annapolis, Maryland, 6-10 July 1998.
2. Wilkerson, T. D., I. Q. Andrus, G. K. Schwemmer, D. O. Miller, Horizontal Wind Measurements using the HARLIE Holographic Lidar, *Proceedings of SPIE Vol.4484 Optical Remote Sensing for Industry and Environment Monitoring II*, San Diego, California, 30-31 July 2001, pp. 64-73.
3. Wilkerson, T. D., C. Q. Egbert, I. Q. Andrus, and M. E. Anderson, Advances in Wind Profiling by Means of Lidar and Video Imagery of Clouds and Aerosols, *Proceedings of SPIE Vol.4723 Laser Radar Technology and Applications VII*, Orlando, Florida, 3-4 April 2002, pp. 130-146.
4. Bilan Energétique du Système Tropical, CNES, 1988.
5. Schwemmer, G. K., Methods and Systems for Collecting Data from Multiple Fields of View, US Patent No. 6,479,808 filed June 28, 2000, awarded Nov. 12, 2002.